

We are IntechOpen, the world's leading publisher of Open Access books Built by scientists, for scientists

6,900

Open access books available

185,000

International authors and editors

200M

Downloads

Our authors are among the

154

Countries delivered to

TOP 1%

most cited scientists

12.2%

Contributors from top 500 universities



WEB OF SCIENCE™

Selection of our books indexed in the Book Citation Index
in Web of Science™ Core Collection (BKCI)

Interested in publishing with us?
Contact book.department@intechopen.com

Numbers displayed above are based on latest data collected.
For more information visit www.intechopen.com



Optimization of Components of Superstructure of High-Speed Rail: The Spanish Experience

Estela Ruiz, Isidro A. Carrascal, Diego Ferreño, José A. Casado and Soraya Diego

Abstract

The performance of rail transport has increased significantly in recent decades, in particular due to the gradual introduction of high-speed rails worldwide. In 1981, the first high-speed line of the world was inaugurated; nowadays, high-speed is operating in more than 20 countries, the high-speed network covering more than 35,000 kms (with more than 25,000 additional kms under construction). Spain is the second country by total distance of railways installed (only behind China) and the first in terms relative to the population and surface. Since the installation of the first high-speed line in Spain in 1992, the elements of the superstructure have undergone a continuous evolution, in order to improve the performance, the durability of the components and the comfort of the passengers. This evolution rests on an adequate selection of materials based on the characterization of their physical and mechanical properties to ensure the optimum in-service conditions. This chapter includes an overview of the different elements present in the railway superstructure of the high-speed lines in Spain. Throughout the text, the innovations incorporated over time are analyzed, as well as the methods used to validate them. In particular, a description of the mechanical characterization procedures is presented.

Keywords: railway, high-speed superstructure, fastening system, mechanical properties, torque, temperature, moisture, corrosion

1. Introduction

Spain occupies the second place in the world, behind China, in kilometers of high-speed railway (HSR) built. The Spanish HSR that links the cities of Madrid and Barcelona was designed to travel at an average speed of 350 km/h in order to compete with the airplane. This implies an increase in average speed of 25% as compared to its predecessor, the railway that connects Madrid and Seville. Consequently, the dynamic forces exerted on the track and all its components have significantly increased.

One of the essential constituent elements that determine the quality of the track is the fastening system that connects the rails and the sleepers which, in turn, transmits both the static and dynamic forces exerted by the passing stocks to the railway infrastructure. Originally, the fastening elements were designed to prevent

the overturning and the transverse displacement of the rails. The advances in railway technology have compelled the fastening systems to fulfill new requirements such as the maintenance of the track gauge or the resistance to longitudinal loads due to the thermal expansion of the welded rails. In addition, the increased use of concrete sleepers has led to the need for the presence of an elastic element between the sleeper and the rail, the rail pads, to cushion the impacts and to reduce the high stiffness of the concrete sleepers.

Currently, the elastic fastening system between rails and sleepers is composed of metal spring clips, insulating plates of a polymeric nature and anchoring screws. These elements fix the rail to the sleeper minimizing the longitudinal and lateral displacements, as well as rotation, that are produced by the transversal, vertical, and longitudinal forces transmitted by the wheels of the passing vehicles. In addition, the fastening system provides the elastic response needed to counteract the vertical wave movements of the track that would give rise to high dynamic forces between wheels and rails avoiding vibrations and noise. Likewise, it maintains the gauge of the track and the inclination of the rails within the admissible tolerances avoiding the overturning of the rail.

The tightening of the fastener that holds the rail to the sleeper plays an essential role in guaranteeing the performance of the whole assembly. In this sense, the grip must provide a resistance to longitudinal displacements higher than the friction between the ballast and the sleeper; in addition, it has to reduce the movements of the head of the rail with a safety coefficient. At the same time, it must withstand the stresses to which it may be subjected to under in-service or accidental conditions. Finally, the electrical insulation between the two rails on electrified lines or equipped with signaling systems must be guaranteed.

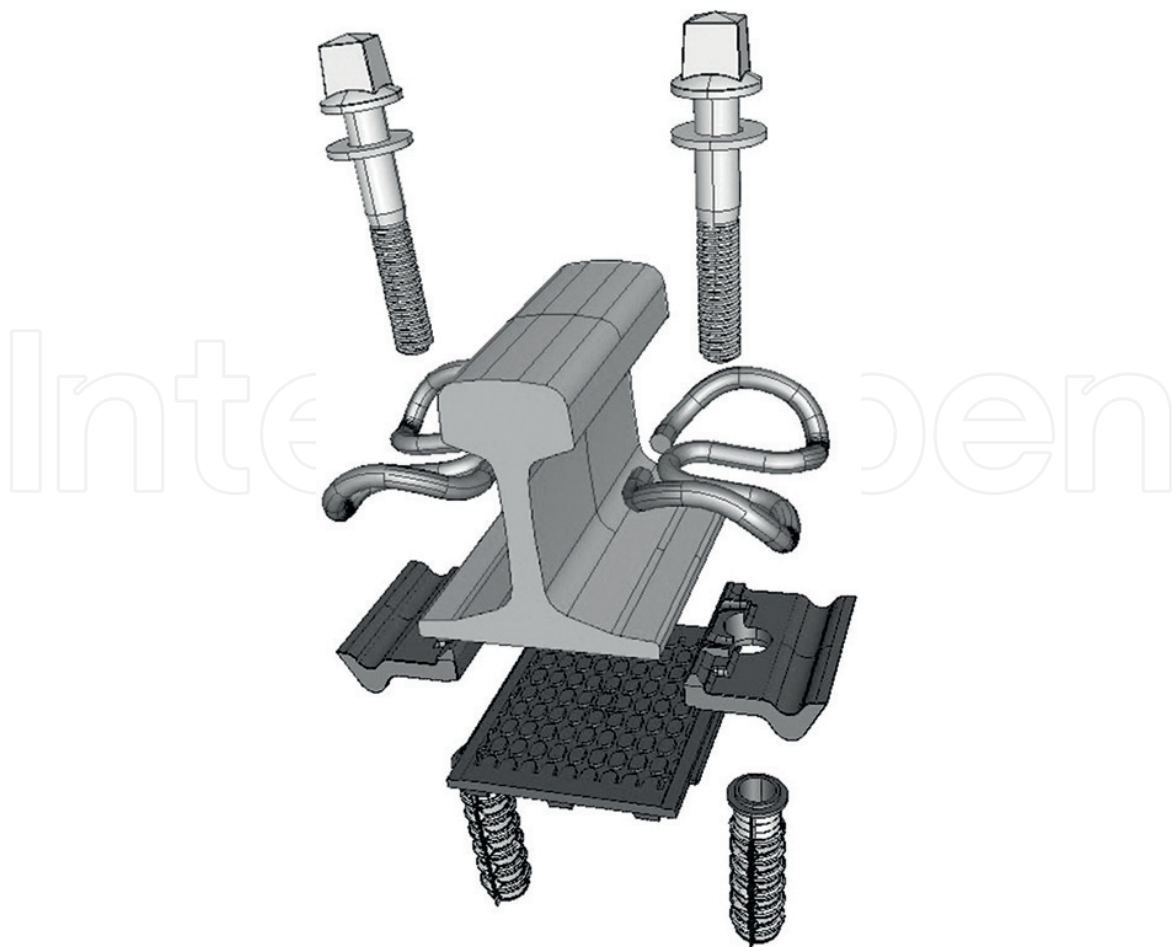


Figure 1.
Sketch of the VM fastening system [2].

Among the existing types, the VM fastening system (see **Figure 1**) is the one installed in the Madrid-Barcelona HSR. Each of the components of this system (tension clips, guide plates, rail pad, plastic dowels, and steel screws) has been optimized regarding its mechanical behavior [1]. This chapter summarizes the studies carried out at LADICIM (Laboratory of Science of Materials of the University of Cantabria) over more than two decades, to improve the mechanical response of each of the constituents of the VM fastening system, in order to optimize the response of the assembly under in-service or accidental conditions. Likewise, the influence of parameters such as the tightening torque on the mechanical response of the system was studied. Finally, the deterioration undergone by the constitutive materials because of the action of external agents (humidity and temperature as a source for corrosion of metals or degradation of polymers) was analyzed in depth.

2. Polyamide guide plates

The mechanical characterization of this type of components is based on the application of three types of loadings: static, impact, and fatigue. In order to optimize this component, an intense experimental campaign has been carried out to analyze the influence of parameters such as the moisture content of the plate, the tightening of the assembly or the mechanical aging of the plate.

For this study, A2-type guide plates injected with polyamide 6.6 reinforced (35% wt.) with short fiber glass were used, all corresponding to the same manufacturing series. The plates were received under the dry-as-molded (DAM) condition after injection and, subsequently, they were subjected to a treatment to gain different moisture contents. A first group remained in an oven at 100°C before testing. At the same time, another group of plates remained in the laboratory environment reaching a moisture content (% wt.) of 0.5%. Three sets of plates were submerged in a water bath at 50°C until reaching humidity contents of, respectively, 1.8, 2.2, and 3.6%. For the characterization of the plates, a specific device setup was developed and manufactured simulating both the support on the sleeper, the fastening system, the tightening of the clip, and the action of the base of the rail.

2.1 Static response

To carry out the tests, an increasing load was applied by means of a universal servo-hydraulic test machine with a loading capacity of ± 250 kN under control of displacement at a speed of 0.05 mm/s. A linear variable displacement transducer (LVDT) was used to record the displacement between the base of the rail and the frame where the guide plate was located.

2.1.1 Influence of the moisture content on the static behavior

To study the influence of the moisture content, plates belonging to each of the groups described above were used. **Figure 2** shows the results obtained in the static test on plates with different degrees of humidity. As can be verified, except for the dry plate which breaks when reaching a certain load value, the rest of the plates present a point of inflection. This phenomenon is due to the fact that increasing the moisture content of the plate increases its deformability and, at some moment in the loading process, the inner part of the hole contacts the screw, and then, they collaborate jointly against the displacement of the rail base.

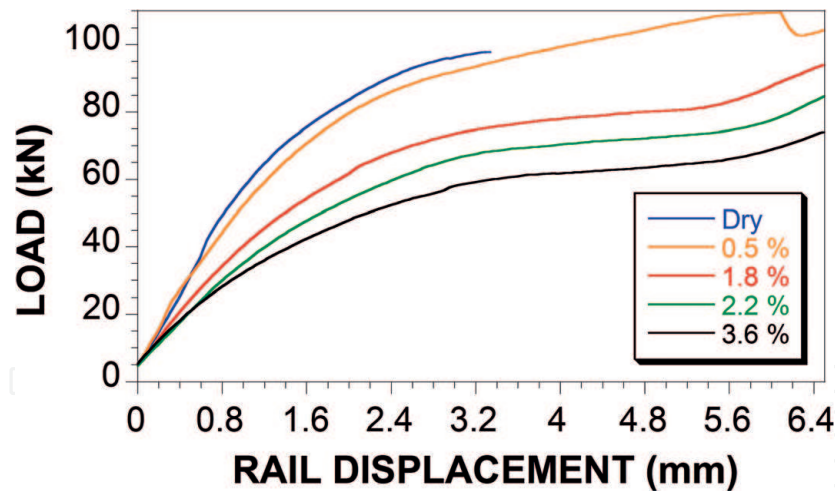


Figure 2.
Results of the static tests conducted on plates with different levels of humidity.

As can be seen in all cases, the contact of the plate with the screw is approximately constant, around 4.4 mm, although, as the plate humidity increases, the force decreases, as the plate becomes more and more flexible.

2.1.2 Influence of the tightening torque on the static behavior

To assess the influence of the tightening torque on the static behavior of the plates, a series of tests was performed applying the following three torques: 100, 250, and 350 N·m. In all cases, plates with a moisture content of 1.8% were employed. The influence of the tightening torque on the static behavior of the plates is represented in **Figure 3**.

As can be appreciated, the curves have the same appearance in the three cases; all the curves show the inflection point that represents the contact point between the plate and the screw. Again, this inflection point occurs for a displacement of 4.4 mm.

On the other hand, the values of the force at the contact point decrease with the tightening torque: 71.4, 79.0, and 80.6 kN for 100, 250, and 350 N·m, respectively. Since the plates have the same moisture content, the fact that the lower the tightening torque, the easier the contact, can be explained because the plate can slide

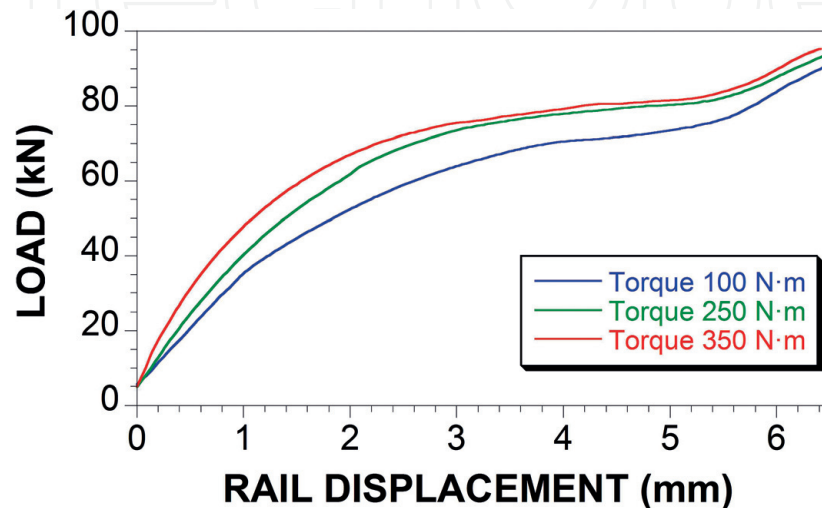


Figure 3.
Influence of the tightening torque on the static behavior of the plate.

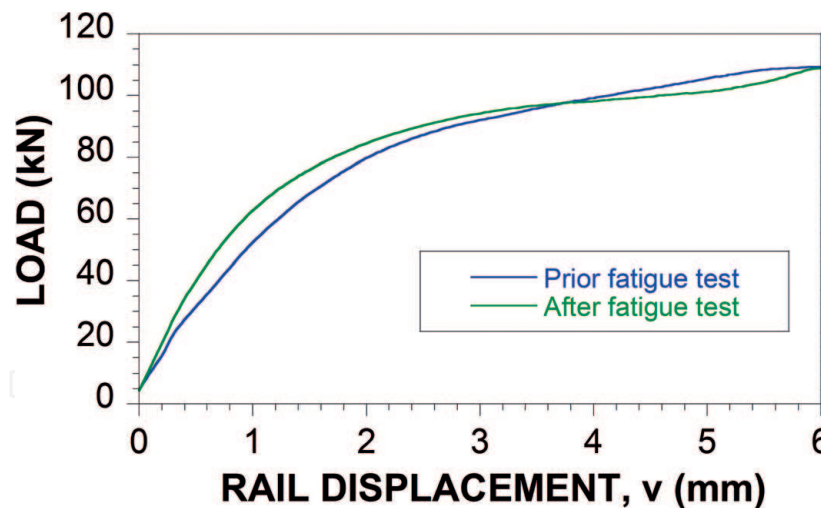


Figure 4.
 Influence of fatigue aging on the static performance of the plates.

more easily with respect to the part that transmits the force. Sliding becomes more difficult as this contact force increases (when the tightening torque is higher).

2.1.3. Influence of fatigue deterioration on the static behavior

The assessment of the influence of fatigue deterioration on the static behavior was carried out on plates with the same humidity, 0.6%, one of them in the original state and the other deteriorated after being subjected to fatigue loading with the following parameters: frequency: 5 Hz, maximum force: 37.7 kN, minimum force: 2.5 kN, and the number of cycles: 500,000. The results can be seen in **Figure 4**, which represents the evolution of these two static tests prior and after fatigue. The behavior of the two plates is similar; the most remarkable difference consists in the greater initial stiffness of the previously fatigued plate; besides, no differences in the values of the contact load can be seen.

2.2 Impact resistance

As in the previous section, the goal of the tests is to determine the influence of variables such as moisture content, tightening torque or fatigue deterioration on the impact resistance of the component. The impact tests were performed applying square wave cycles under control of displacement conditions with sufficient amplitude to provoke the failure of the plate.

2.2.1 Influence of the moisture content on the impact resistance

To study the influence of the moisture content on the behavior under an impact loading, plates with the following humidity contents were used: dried in an oven, 0.5, 1.8, 2.2, and 3.6%. The results obtained after the impact tests of plates with different degrees of humidity are represented in **Figure 5**. The first remarkable difference with the static response is that the failure of the plates occurs in all cases before the contact with the screw. Only the plate with a moisture content of 3.6% may raise a doubt because its displacement slightly exceeds the limit of 4.4 mm established previously; nevertheless, since there is no change in the slope of the curve nor any type of mark on the plate after test, the contact with the screw can be discarded.

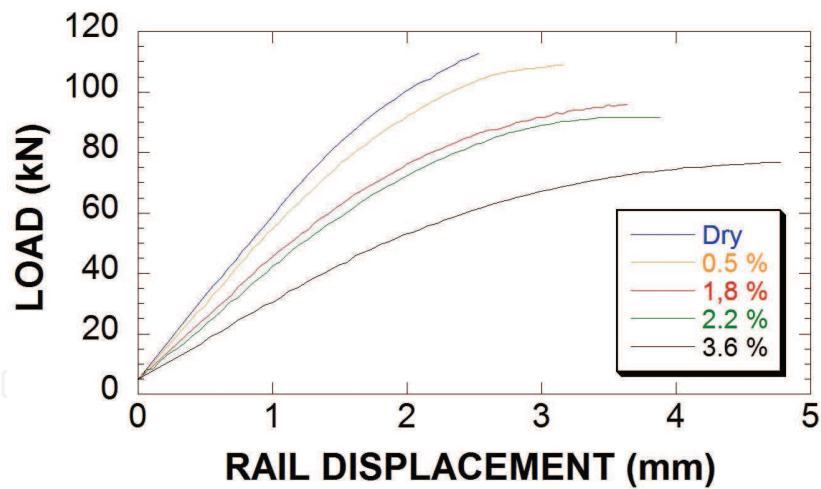


Figure 5.
Results of the impact tests on plates with different moisture contents.

The above figure makes it possible to draw the following additional conclusions: the stiffness of the plates increases as the moisture content decreases; notice that this pattern was also observed for the static tests. Moreover, the deformation at fracture increases with humidity, whereas the maximum force decreases.

2.2.2 Influence of the tightening torque on the impact resistance

To study the influence of the tightening torque, the same tests were carried out as in the static study, that is, the three following tightening torques were applied on dry plates: 100, 250, and 350 N·m, respectively. In **Figure 6**, the force-displacement curves of the three tests are shown. As can be seen, the plates show a stiffer behavior when the tightening torque is increased (as occurred for the static behavior); moreover, increasing the torque also increases the maximum force and decreases the deformation. This can be explained on the basis that, as the torque decreases, the contact force on the plate decreases too, facilitating the sliding of the plate and therefore its displacement.

2.2.3 Influence of fatigue on the impact resistance

To finish the study on the impact resistance, the influence of the deterioration due to fatigue was studied. The experiment was carried out on plates with a

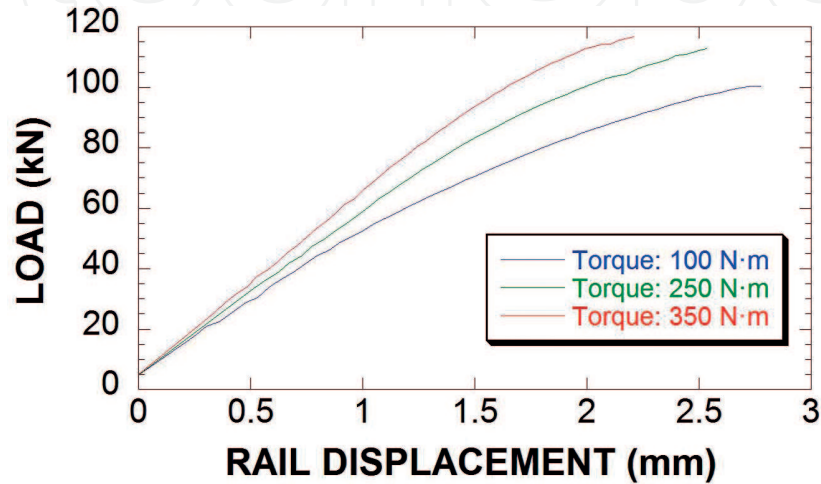


Figure 6.
Influence of the tightening torque on the impact behavior of the plate.

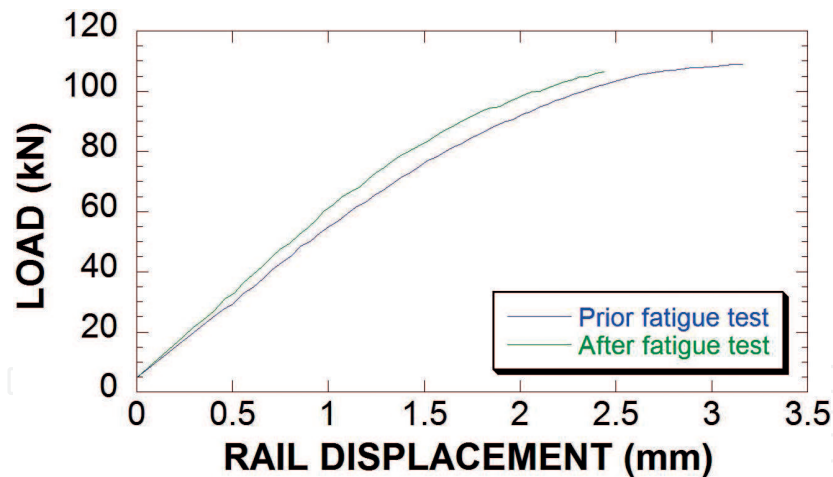


Figure 7.
Influence of the fatigue aging on the impact resistance.

humidity of 0.6% that were subjected to 500,000 sinus-type cycles with the parameters described above. The results are represented in **Figure 7**, where the load-displacement curves of two impact tests are shown, one performed on an original plate and the other on a fatigue-aged plate. The graph shows that fatigue aging by fatigue tends to stiffen the plate, decreasing the deformability at fracture by more than 0.5 mm without affecting the fracture load.

2.3 Fatigue behavior

In this section, the behavior of the plate subjected to dynamic cyclical loads will be studied. In addition, the influence on this behavior of external parameters, such as the moisture content of the plate or the value of the tightening torque applied to the clamping assembly will be assessed. For the fatigue characterization, the Locati test technique [3–5] was used; this consists in applying blocks (composed of a constant number of cycles) of increasing maximum load, starting from a value lower than the fatigue limit. At a certain level of maximum load, the maximum strain grows rapidly, preceding the failure of the plate.

2.3.1 Influence of the moisture content on the fatigue behavior of the plate

For this analysis, the Locati method was used applying loading blocks of 20,000 square wave cycles with a frequency of 5 Hz; the load for the initial block ranged between 5 and 45 kN. The minimum value was kept constant throughout the whole test, while the maximum load value was increased by 2 kN in each block. **Table 1** and **Figure 8** show, as a summary, the results obtained in the Locati tests carried out

Humidity (%)	Critical block	$\Delta\sigma_e$ (kN)	T_c (°C)	Cycles to failure
3.6	2	40	42	98,887
2.2	3	42	44	119,508
1.8	5	46	46	129,057
0.6	6/7	48	48.5	153,929
0	10/11	56	52	229,297

Table 1.
Influence of the moisture content on the fatigue behavior of the plates.

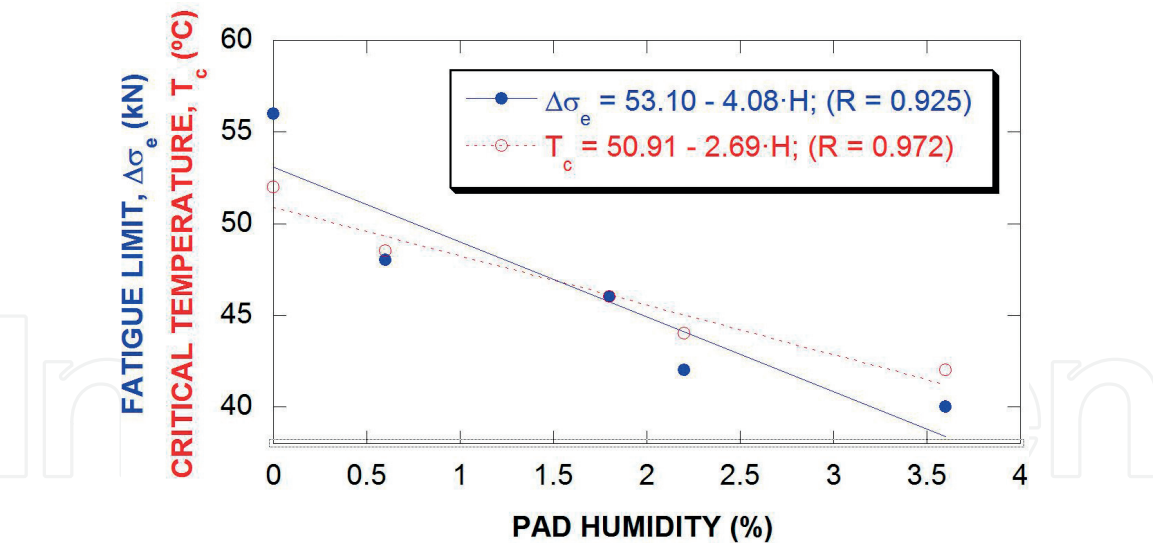


Figure 8.
Influence of moisture content on fatigue limit and critical temperature.

on plates with different moisture contents, verifying how the fatigue limit, $\Delta\sigma_e$, increases with the decrease in the moisture content of the plate. In the same figure, the evolution of the critical temperature, T_c , for the different moisture contents is represented, obtaining the same decreasing relation.

The dry plates under static loading failed in a brittle manner, as opposed to the ductile failure of the wet plates. In contrast, under impact conditions, both types of plates exhibit a brittle response. Finally, the fracture of the plates under fatigue loading is ductile in all cases, regardless of the level of moisture content.

2.3.2 Influence of the tightening torque on the fatigue behavior of the plate

As in the static and impact cases, the tightening torque applied in the fastening system may modify the fatigue behavior of the plate. To verify the influence of this parameter, Locati tests were carried out on plates with the same moisture content (0.6%) varying the tightening torque according to the following values: 100, 250, and 350 N·m. The parameters chosen in the Locati tests were the same as those described before. The increase in the tightening torque improves the fatigue behavior of the plate. **Table 2** and **Figure 9** show, as a summary, the results obtained in the Locati tests carried out on plates with different tightening torques and moisture contents.

As can be seen, as far as fatigue is concerned, increasing the tightening torque has similar consequences as reducing the moisture content. It can be concluded that the critical temperature depends not only on the material but also on the certain boundary conditions, in this case, on the tightening torque of the assembly.

Torque (N·m)	$\Delta\sigma_c$ (kN)	T_c (°C)	Critical block	Cycles to failure
100	44	41.5	60,000-80,000	107,832
250	48	48.5	100,000-140,000	153,929
350	52	52	140,000-180,000	196,377

Table 2.
Influence of tightening torque on the fatigue behavior.

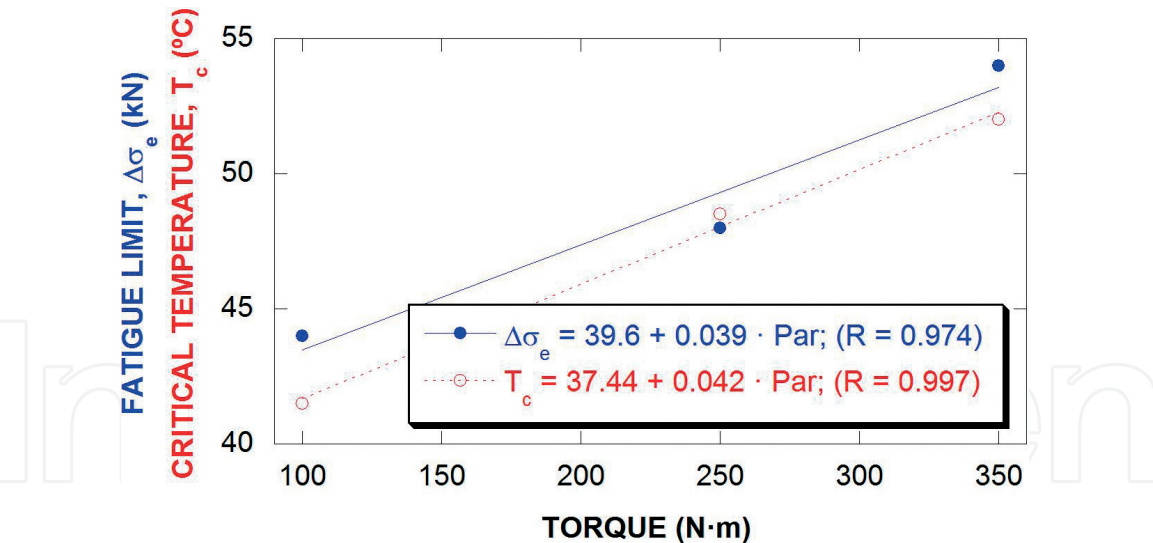


Figure 9.
Influence of the tightening torque on the fatigue behavior of the plate.

3. Rail pad

The rail pads used were made of thermoplastic elastomer (TPE) with a nominal stiffness of 100 kN/mm. As a new track is subjected to the repetitive loads caused by the passage of the trains, it suffers plastic deformations that grow until the system reaches the steady state and the material responds in a true elastic manner.

It has been verified [6, 7] that a high value of the stiffness of the rail pad increases the dynamic overloads due to the nonsuspended masses, accelerating the deterioration of the track, while a low value causes an excessive displacement of the track with a significant increase in the rail stresses. Therefore, it is necessary to delimit the validity interval of the stiffness. In the technical specification for the supply of fasteners of the GIF [8], both static and dynamic stiffness values are delimited. The value of the static vertical stiffness, k_s , must be included in the interval $80 \leq k_s \leq 125$ kN/mm, while the dynamic stiffness value, k_d , must belong to the interval $k_s \leq k_d \leq 2 k_s$. Due to the nature of the constituent material of the pads, stiffness may be modified by different environmental agents such as temperature, which can fluctuate in track between -20 and 80°C , humidity or deterioration suffered by the pads due to the continued mechanical stresses of compressive fatigue [9]. In this section, the influence of these variables on the stiffness of the pads has been measured, in order to identify the conditions leading to the nonfulfillment of the above-mentioned requirements.

3.1 Influence of the temperature on the static behavior

The evaluation of the static behavior was determined from static stiffness tests (20/95 kN), applying a vertical load to the rail pad by means of the specific device. This device simulates the in-service working conditions, where the load was applied by means of a rail coupon, equipped with a ball joint that ensured the verticality of the loads. The mean vertical descent of the rail with respect to the support tool registered by four LVDTs (range: ± 5 mm), located in each of the corners of the support, was considered as the strain index of the rail pad. The load was applied by means of an actuator with a loading capacity of ± 250 kN. The influence of temperature on the behavior of the rail pad was evaluated by introducing the device into an environmental chamber adapted to the test machine. Measurements of Shore D

hardness [10] were carried out, aimed at finding a correlation of this parameter with the evolution of the mechanical behavior of the rail pad. The vertical static stiffness tests were carried out according to the provisions indicated in the technical specification [8] using a clamping force of 20 kN. The static behavior of rail pads at different temperatures (-10, 20, 50, and 80°C) was studied. In the graph of **Figure 10**, the evolution of the shortening of the rail pad in the third load-unload cycle at temperatures of -10, 20, 50, and 80°C can be seen.

The rail pad shortening ranges from maximum values of 0.93 mm at 80°C to a minimum of 0.59 mm at -10°C.

In **Figure 11**, the stiffness and the hardness of the rail pad versus temperature are represented in the double axis. An inverse linear correlation between static stiffness (20/95 kN) and the Shore D hardness with the rail pad temperature is shown; in summary, an increase in temperature causes the softening of the rail pad. An increase of 90°C in the test temperature, from -10°C, generates a 44% decrease in the stiffness of the rail pad (from 128 kN/mm to 80 kN/mm at 80°C). The decrease in Shore D hardness is less noticeable (from 43.6 to 39.6) which is a decrease of 9.5% compared to the room temperature. The stiffness value is between

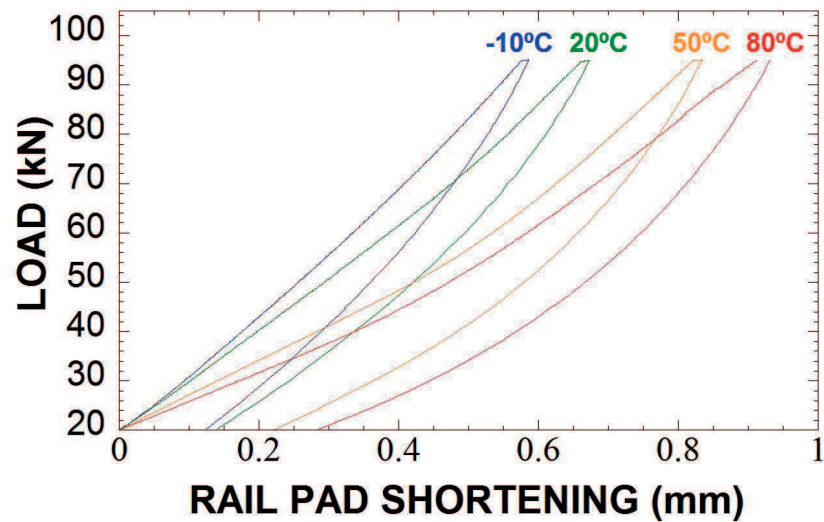


Figure 10.
Static behavior of the rail pad at different temperatures.

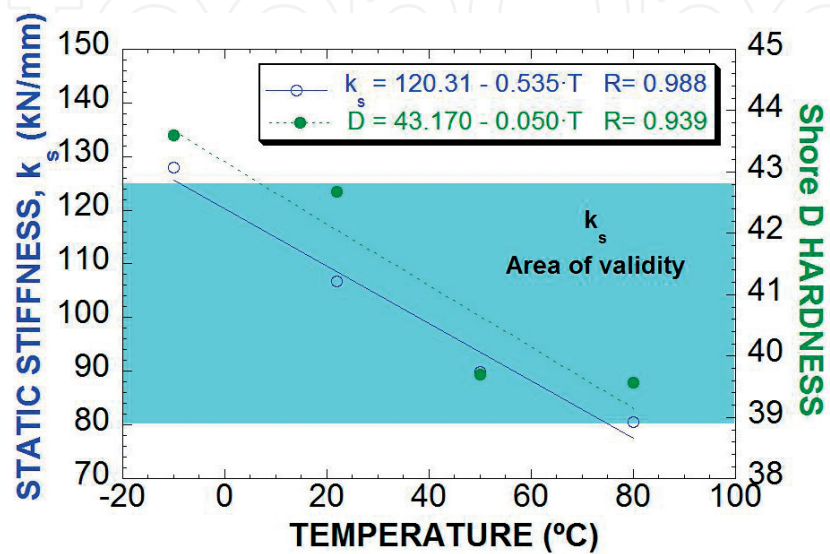


Figure 11.
Evolution of the stiffness and hardness of the rail pad with the temperature.

the established limits (80–125 kN/mm), except for the extreme temperature values 128.0 kN/mm to -10°C and 80.6 kN/mm to 80°C .

3.2 Influence of temperature on the dynamic behavior

The influence of temperature on the dynamic behavior was measured through dynamic stiffness tests at low frequency. The test consists in applying 1000 load cycles of a sinusoidal nature between 20 and 95 kN at a frequency of 5 Hz, determining the stiffness as the average obtained in the last 10 cycles. The dynamic stiffness was analyzed at different temperatures: 20, 40, 60, and 80°C . In **Figure 12**, the evolution of the shortening of the rail pad during the last cycle is represented. The differences with respect to the previous static behavior are appreciated. Thus, the rail pad only shortens by 0.64 mm at 80°C under dynamic conditions, having reached a 31.2% higher static strain. This decrease in the strains also reflects a decrease in the dynamic energy dissipated (E_{dd}); thus, the material under dynamic conditions resembles an elastic body that does not dissipate energy (**Figure 13**).

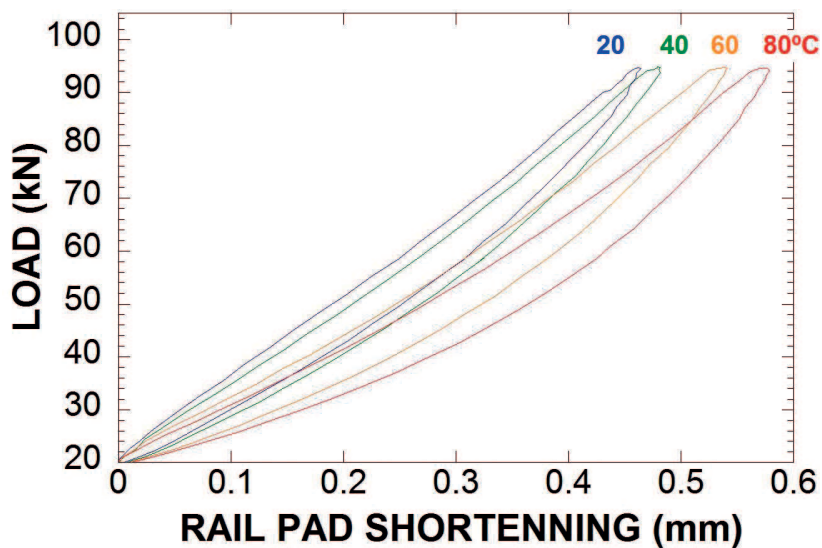


Figure 12.
Dynamic behavior at different temperatures (cycle 1000).

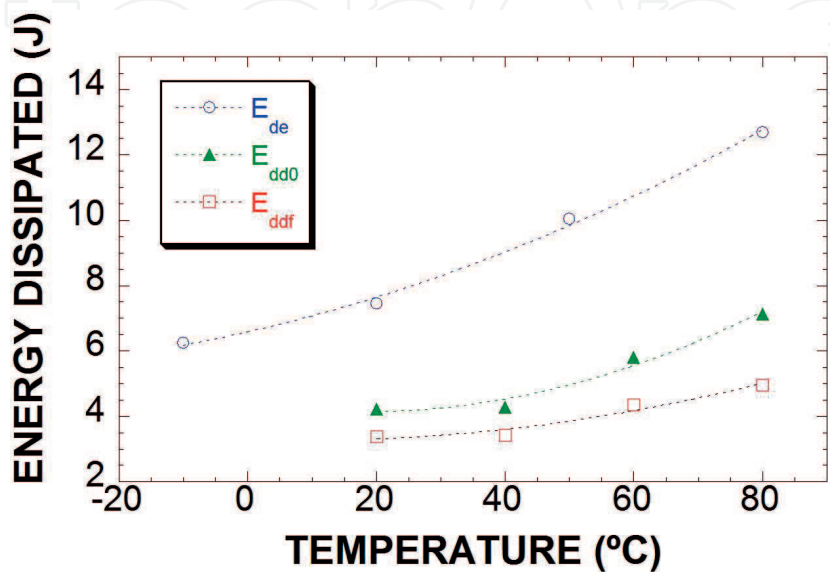


Figure 13.
Energy dissipated under static conditions (E_{de}) and dynamic (E_{dd}).

4. Anchorage components

The study of the anchor was separated into two parts: on the one hand, the polymer dowel was analyzed, studying its mechanical behavior under static and dynamic regimes; on the other hand, the metallic screw was subjected to loading configurations (tensile, bending, and impact) similar to those suffered under actual in-service conditions.

4.1 Dowel

The dowel consists of two components, namely, the main body made of polyamide 6.6 reinforced with glass fiber (30% wt.) and the metal sheet that surrounds the core peripherally. Due to the hygroscopic nature of the polyamide, the following treatments were applied to obtain a series of dowels with different moisture contents in order to know the influence of this parameter on the mechanical behavior:

- Drying in an oven at 100°C for 1 year.
- Maintaining the laboratory environment for 1 year.
- Immersion in water at room temperature for 3 months and then maintained in the laboratory environment for 9 months.
- Immersion in water at room temperature for a year.

These types of treatments were aimed at simulating the worst conditions that may take place in the preparations of the sleepers.

The moisture contents obtained with the different treatments were determined in two different ways. On the one hand, the overall content was measured weighing the dowel before and after the treatment and, on the other hand, the moisture content of the thread was calculated once it had been removed from the dowel in the mechanical tests and weighing the same before and after placing it in an oven for 7 days at 100°C. The latter procedure provides more representative values, since it is being measured in the resistant zone of the component. In addition, the humidity of the thread is, in all cases, higher than the overall humidity, since it is an area with greater external surface, and the water is absorbed more easily, being lighter in the last two treatments, since the interior area is the one that was in direct contact with the water that contained the dowel. The results obtained from the different moisture contents are shown in **Table 3**.

The critical stresses that the anchor must support are, mainly, parallel to the axis of the dowel-screw assembly, that is to say, forces that pull the screw out of the dowel. Therefore, the tool designed for the mechanical characterization of the dowels

Treatment	Total moisture (%)	Moisture thread (%)
1 year, dry in stove	0.00	0.00
1 year, environment	1.08	1.54
3 months, submerged in water	1.43	1.90
1 year, submerged in water	2.60	4.80

Table 3.
Humidity of the dowel according to the treatment.

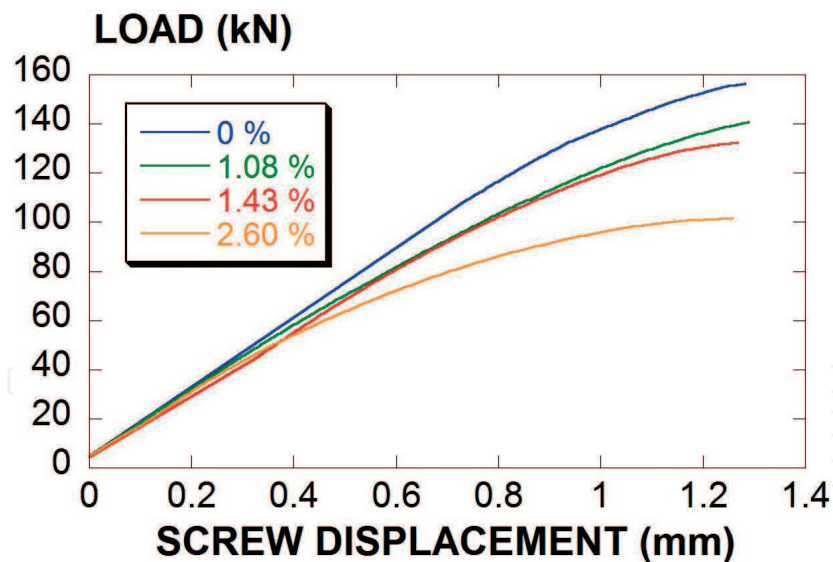


Figure 14.
 Static test on dowels.

simulated this type of loading conditions. The characterization was based on both static and dynamic regimes, where the last one includes impact and fatigue efforts.

4.1.1 Characterization of the dowels under static loading

For the static characterization of the dowels, the load screw was driven to a depth of 64 mm, similar to the in-service position; then, an extraction force was applied until fracture at a loading rate of 1 kN/s. The results obtained on the dowels subjected to the different moisture treatments are represented in **Figure 14**. In view of the results, it is verified that the breaking load, as well as the initial stiffness of the component, increases as humidity decreases, while the deformation at fracture remains approximately constant. Therefore, the energy at failure decreases with increasing humidity. The constant value of the displacement at failure is explained because the applied stress is distributed uniformly along 14 thread passages, provoking the fracture of all of them simultaneously by shearing. As can also be seen, even for the highest moisture content, the limit value imposed by the technical specification (60 kN) is exceeded.

4.1.2 Characterization of the dowel under impact loading

In this case, the screw was driven to a depth of 64 mm and then a square wave cycle was applied to provoke the fracture of the component. The results obtained for the dowels subjected to the different moisture treatments appear in the graph of **Figure 15**, and these values are higher than those obtained in the static tests, while deformation increases with humidity, until reaching values similar to those obtained under static conditions. In the case of the two dowels with the lowest moisture content, fracture occurred at the depth where the screw thread reaches, this being the reason that explains why the fracture deformations of the dry samples were slightly lower than those of the wet ones.

The results allow it to be verified that the fracture load increases as the humidity decreases, characterization of the dowels under fatigue loading.

The Locati methodology was employed for fatigue characterization. Blocks of 20,000 square wave cycles were applied at a frequency of 5 Hz, with an initial loading range between 5 and 50 kN. The minimum load was constant during the

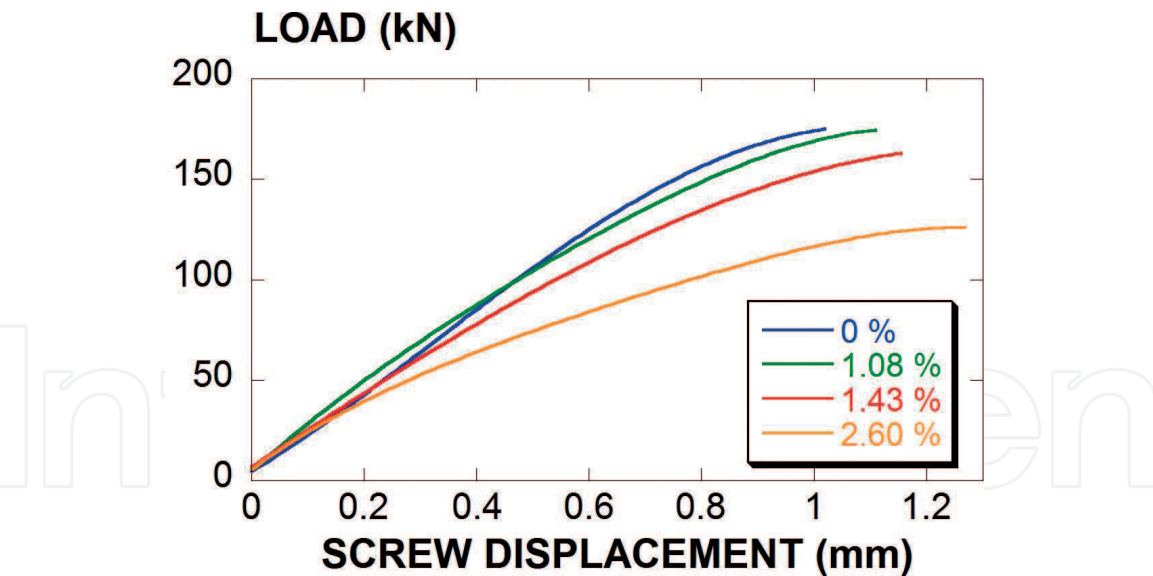


Figure 15.
Impact test on dowels.

test, while the maximum value was increased by 2 kN in each block. The results obtained in this experiment cannot be used to be compared with different tests because a nonquantified relative displacement between the dowel and the screw took place. The analysis of the displacement variation versus the number of cycles was used to determine the critical block. The results summarized in **Table 4** are obtained from dowels with different moisture contents in order to determine the critical parameters of fatigue.

The strong influence of moisture content on the fatigue behavior of this material is verified; note that the fatigue resistance of the dry dowel changes from 74 to 52 kN in the case of the wet dowel. The requirement of the technical specification regarding the extraction of fasteners is 60 kN in static regime; therefore, the fatigue limit exceeds this condition in all cases but for the case of maximum humidity.

4.2 Screw

The mechanical characterization was carried out following the requirements indicated by the internal control standard of the supplier [11]. The properties characterized were tensile, bending, and impact strength. Screws were used in the as-received state and were subjected to accelerated corrosion for 300 hours in a salt spray chamber to evaluate the influence of the exposure to a corrosive environment on the mechanical properties.

Humidity (%)	Critical Step	Critical F. (kN)	$\Delta\sigma_e$ (kN)	Critical number of cycles	Breakage n ^o of cycles
0/0	14	76	74	260-280·10 ³	321,101
1.08/1.54	12	72	70	220-240·10 ³	281,961
1.43/1.90	10	68	66	180-200·10 ³	251,072
2.60/4.80	3	54	52	40-60·10 ³	87,989

Table 4.
Summary of the results obtained in the Locati tests.

4.2.1 Tensile characterization

For the tensile characterization, a specific setup was designed and manufactured. Deformations were recorded by means of an extensometer with a gauge of 12.5 mm placed on two of the fillets of the screw. This layout allows the possible failure of the head of the screw to be assessed. Tests were carried out on a screw in the as-received condition as well as on two of the screws previously submitted to the salt spray chamber, one of which had even suffered a small notch in the bottom of a fillet, in order to accelerate the corrosion process. The graph of **Figure 16** shows the results of the tensile tests performed on the three samples, and the parameters obtained in each of the tests are summarized in **Table 5**. As can be seen, the effect of exposure in the salt spray chamber has not penalized the tensile mechanical behavior of the screw. Even the notch has had little influence, since the failure occurred in a different cross section.

4.2.2 Bending characterization

The bending test consisted in obtaining, respectively, a permanent angle of 15 and 30°, verifying the integrity of the sample when bending over a 40 mm radius. As in the previous case, the test was carried out on a sample in the as-received condition and on another one that had remained 300 hours in a salt spray chamber. After applying a bending of 15°, no visible defects appeared in any of the screws. With the 30°, small cracks can be seen in both samples; consequently, no differences are appreciated between samples regarding the bending ability. **Figure 17** shows the appearance of the samples tested after bending 30°.

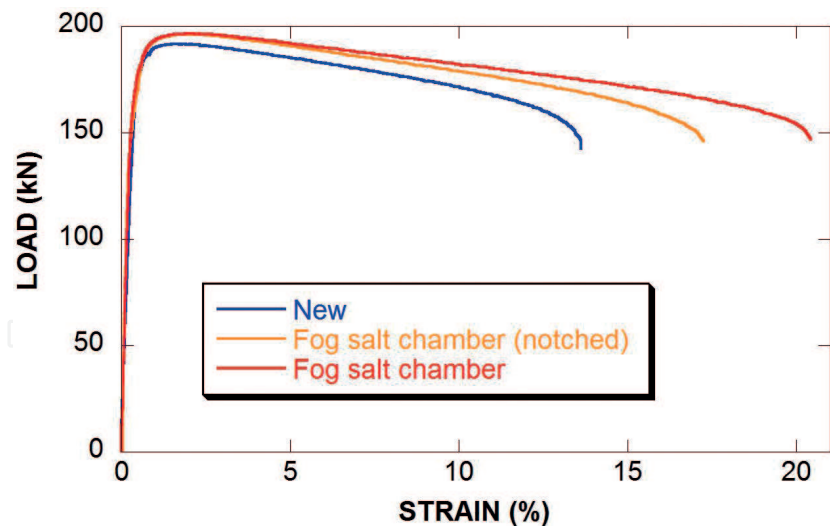


Figure 16.
Tensile test on the screws.

Screw	Maximum force (kN)	Strain under Max. Force (%)	Cross section reduction (%)
New	191.7	1.80	13.65
Fog salt chamber (notched)	196.2	1.96	14.13
Fog salt chamber	196.6	2.02	12.56

Table 5.
Parameters obtained in tensile tests.



Figure 17.
Appearance of the samples after the bending test.

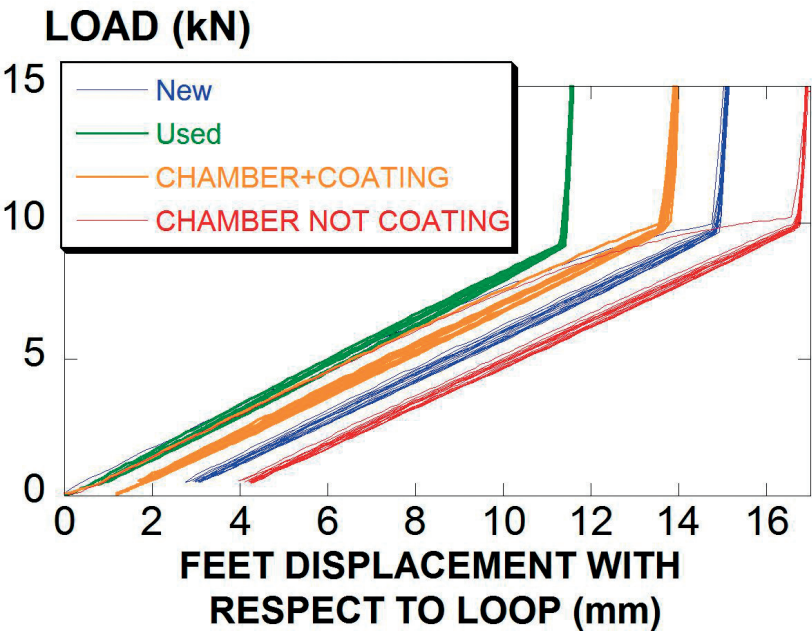


Figure 18.
Load cycles on clip.

5. SKL-1 clip

This part of the study was aimed at assessing the loss of mechanical performance of the clip SKL-1 depending on the degree of use. New clips, clips used under normal and extraordinary conditions, and clips subjected to different deterioration treatments were used. To simulate in-service conditions, a compressive load of 15 kN was applied for 10 s, and the sample was unloaded to 0.5 kN; this sequence was repeated nine more times. **Figure 18** shows the experimental curves obtained from the clips previously described. The comparison of responses was carried out using clips subjected to the following different conditions:

- New clip, not previously tightened.
- Used clip, tightened 22 times with a torque of 250 N·m and then three times with 350 N·m.

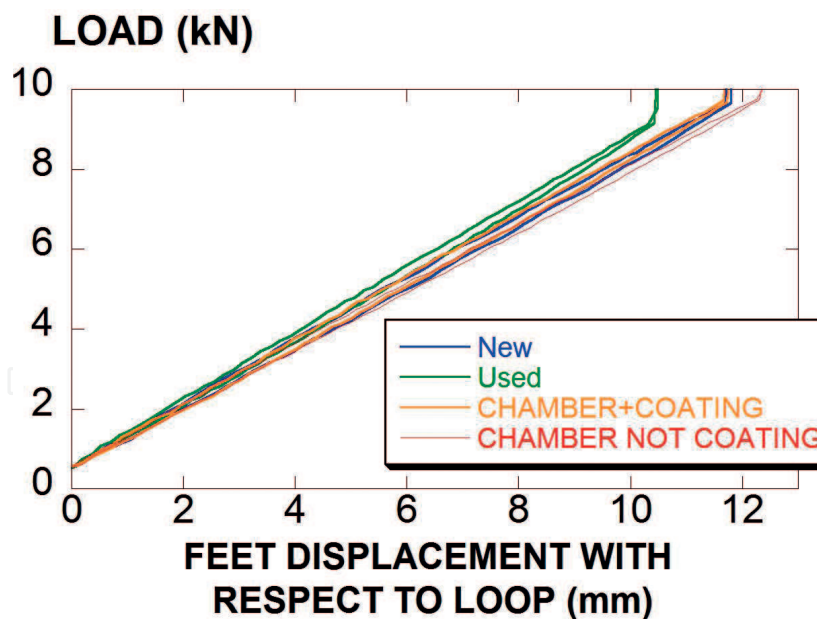


Figure 19.
 Detail of the last load cycle on clip.

- Clip with coating introduced in a salt fog spray chamber for 300 hours and with a pretightening of 250 N·m.
- Uncoated clip inserted in salt fog spray chamber for 300 hours without tightening.

The difference between the first cycle and the rest of them was analyzed. The used clip was the only one in which this difference did not occur, since it behaved elastically from the first cycle. The clips that had not been previously tightened show a first cycle with higher compliance and permanent deformation. In addition, in the case of the salt chamber clip without coating, the flexibility is greater than in the new one, possibly due to the loss of net section because of the corrosion process. In all cases, the following cycles do not show plastic deformations. **Figure 19** shows a detail of the last 10 load cycles applied to the four clips.

The highest stiffness corresponds to the clip used, and the greatest flexibility to the clip subjected to the salt chamber without coating. As for the new clip and the salt chamber with coating, the difference between them is negligible, showing a behavior in an intermediate situation between the previous ones.

6. Conclusions

The increase in speed and the improvements in comfort and safety experienced by the high-speed train in recent decades are the result of the engineering innovations implemented in this means of transportation. In this chapter, the studies developed by the LADICIM research group on the design of the fastening system between the sleeper and the rail have been examined. Once verified that the fastening system selected for the high-speed line between Madrid and Barcelona fulfills the requirements of the European standards EN 13146, this contribution focuses on the experimental results derived from the characterization of each of its components. The conclusions drawn from this research are summarized hereafter:

- Guide plate

Increasing the moisture content reduces the strength and increases the deformability of the plate. This reduces the static force to be applied to provoke the contact with the screw. In case of an impact, the plate fails before contacting the screw, and fracture occurs with greater deformation and less force when the moisture content increases. This increase also causes a decrease in fatigue resistance.

The increase of the tightening torque applied to the system raises the force required to achieve the plate-screw contact under static conditions, reduces the impact deformability, and increases the resistance against fatigue.

A plate tested for 500,000 cycles has approximately the same behavior under static and impact conditions as an original plate.

- Seat pad

Temperature reduces the stiffness of the plate, both under quasi-static or dynamic conditions. The energy dissipated per cycle is accentuated by increasing the temperature.

Hardness correlates linearly with stiffness; then, hardness can be considered as an index of the degree of degradation undergone by the pad. This parameter is very useful as it can be easily measured by a nondestructive test on the track under in-service conditions.

Extreme temperature values on the railway track (-20 and 80°C) define the threshold working values for seat pads, both under dynamic and static conditions.

- Anchorage components

Increasing the humidity content of the dowel reduces the resistance under static, impact, and fatigue loading. Even in the worst scenario, this component fulfills the minimum requirements imposed by the European standard.

The screw subjected to saline fog chamber for 300 h shows a tensile behavior very similar to an original screw; the presence of a small notch does not reduce its mechanical resistance. In both cases, the screw survived to the bending test.

- Clip

The only difference between a used clip, a new one or one subjected to 300 h in a saline fog chamber lies in the first loading cycle; once the component is plasticized, the behavior is similar.

IntechOpen


IntechOpen

Author details

Estela Ruiz, Isidro A. Carrascal, Diego Ferreño*, José A. Casado and Soraya Diego LADICIM (Laboratory of Science and Engineering of Materials), University of Cantabria, E.T.S. de Ingenieros de Caminos, Canales y Puertos, Santander, Spain

*Address all correspondence to: diego.ferreno@unican.es

IntechOpen

© 2018 The Author(s). Licensee IntechOpen. This chapter is distributed under the terms of the Creative Commons Attribution License (<http://creativecommons.org/licenses/by/3.0>), which permits unrestricted use, distribution, and reproduction in any medium, provided the original work is properly cited. 

References

- [1] Carrascal IA. Optimización y análisis de comportamiento de sistemas de sujeción para vías de ferrocarril de alta velocidad española [thesis]. Santander: University of Cantabria; 2010
- [2] Soluciones M. Fastening systems [Report]. 2009
- [3] Locati L. La Fatica dei Materiali Metallici. Milano: Ulrico Hoepli; 1950
- [4] Locati L. Programmed fatigue test, variable amplitude rotat. La Metallurgia Italiana. 1952;44(4):135-144
- [5] Casado JA, Polanco JA, Carrascal I, Gutiérrez-Solana F. Application of the locati method to material selection for reinforced polymeric parts subjected to fatigue. In: International Conference on Fatigue of Composites. Paris. Proceedings of the Eighth International Spring Meeting. June 1997. Issue 8. pp. 454-461. <http://www.worldcat.org/title/international-conference-on-fatigue-of-composites-conference-internationale-sur-la-fatigue-des-composites-eight-international-spring-meeting-huitiemes-journees-internationales-de-printemps-paris-3-4-5-june-1997/oclc/496942402>
- [6] Lopez Pita A. La rigidez vertical de la vía y el deterioro de las líneas de alta velocidad. Revista de obras públicas; November 2001. Issue 3415. pp. 7-26. http://ropdigital.ciccp.es/revista_op/detalle_articulo.php?registro=18223&anio=2001&numero_revista=3415
- [7] Carrascal IA, Casado JA, Polanco JA, Gutiérrez-Solana F. Dynamic behaviour of railway fastening setting pads. Engineering Failure Analysis. 2007; 14(2):364-373
- [8] EN13481-2:2012+A1:2017, Railway applications. Track. Performance requirements for fastening systems. Part 2: Fastening systems for concrete sleepers, and EN 13481-5:2012+A1:2017, Railway applications. Track. Performance requirements for fastening systems. Part 5: Fastening systems for slab track with rail on the surface or rail embedded in a channel
- [9] Carrascal IA, Casado JA, Polanco JA, Gutiérrez-Solana F. Comportamiento dinámico de placas de asiento de sujeción de vía de ferrocarril. Anales de mecánica de la fractura. Vol. XXII. 2005. Almagro. <http://www.gef.es/web/Publicaciones.asp>
- [10] UNE-EN ISO 868. Plásticos y ebonitas. Determinación de la dureza de indentación por medio de un durómetro. (Dureza Shore); 2003. https://books.google.es/books/about/UNE_EN_ISO_868_2003_pl%C3%A1sticos_y_ebonita.html?id=F46MswEACAAJ&redir_esc=y
- [11] Technical Specification ET 03.360.572.6 B080805, Anclaje tipo Plastirail. ADIF (Spanish Administrator of Railway Infrastructures)